16:01:31 OCA PAD AMENDMENT - PROJECT HEADER INFORMATION 09/22/94

Active

Project #: E-16-X39 Cost share #: E-16-384 Rev #: 1
Center # : 10/24-6-R8160-0A0 Center shr #: 10/22-1-F8160-0A0 OCA file #:
Work type : RES
Contract#: 42-950055-59 Mod #: 1 Document : CONT
Prime #: NAS3-25982 Contract entity: GTRC

Subprojects ? : N CFDA:
Main project #: PE #:

Project unit: AERO ENGR Unit code: 02.010.110
Project director(s):
KOMERATH N M AERO ENGR (404)894-3017

Sponsor/division names: SAIC /
Sponsor/division codes: 218 / 001

Award period: 940602 to 950105 (performance) 950105 (reports)

Sponsor amount	New this change	Total to date
Contract value	10,652.00	18,357.00
Funded	10,652.00	18,357.00
Cost sharing amount		3,041.00

Does subcontracting plan apply ?: N

Title: PULSED AIR JET FLOW DEFINITION

PROJECT ADMINISTRATION DATA

OCA contact: Brian J. Lindberg 894-4820

Sponsor technical contact

DR. YOUSEF BAHADORI
(310)781-8723

SAIC
21151 WESTERN AVENUE
TORRANCE, CA 90501-1724

Sponsor issuing office

SUSAN DEPTULA
(619)535-7125

SAIC
10260 CAMPUS POINT DRIVE
SAN DIEGO, CA 92121-1578

Security class (U,C,S,TS) : U ONR resident rep. is ACO (Y/N): N
Defense priority rating : N/A N/A supplemental sheet
Equipment title vests with: Sponsor X GIT
HOWEVER, NONE PROPOSED OR ANTICIPATED.
Administrative comments -
CHANGE ORDER NUMBER 01 ADDS $10,652 IN NEW FUNDS AND EXTENDS PERIOD OF PERFORMANCE THROUGH JANUARY 5, 1995. TOTAL FUNDING NOW: $18,357.

GEORGIA INSTITUTE OF TECHNOLOGY
OFFICE OF CONTRACT ADMINISTRATION

NOTICE OF PROJECT CLOSEOUT

Closeout Notice Date 01/05/95

Project No. E-16-X39 Center No. 10/24-6-R8160-0A0

Project Director KOMERATH N M School/Lab AERO ENGR

Sponsor SAIC/

Contract/Grant No. 42-950055-59 Contract Entity GTRC

Prime Contract No. NAS3-25982

Title PULSED AIR JET FLOW DEFINITION

Effective Completion Date 950105 (Performance) 950105 (Reports)

Closeout Actions Required:	Y/N	Date Submitted
Final Invoice or Copy of Final Invoice	Y	
Final Report of Inventions and/or Subcontracts	Y	
Government Property Inventory & Related Certificate	Y	
Classified Material Certificate	N	
Release and Assignment	Y	
Other	N	

Comments

Subproject Under Main Project No.

Continues Project No.

Distribution Required:

Project Director	Y
Administrative Network Representative	Y
GTRI Accounting/Grants and Contracts	Y
Procurement/Supply Services	Y
Research Property Managment	Y
Research Security Services	N
Reports Coordinator (OCA)	Y
GTRC	Y
Project File	Y
Other	N
	N

NOTE: Final Patent Questionnaire sent to PDPI.

Technical Report on Subcontract 42-950055-59

PULSED AIR JET FLOW DEFINITION

Work Performed at
GEORGIA INSTITUTE OF TECHNOLOGY
SCHOOL OF AEROSPACE ENGINEERING
ATLANTA, GEORGIA 30332-0150

Research Team:
Bryce Roth , Urmila Reddy, Robert Funk
Narayanan Komerath (Principal Investigator),
School of Aerospace Engineering, Georgia Institute of Technology

SAIC Technical Monitors: Drs. Yousef Bahaduri and Uday Hegde

GITAER-EAG-94-8
December 1994

Table of Contents

Abstract

A pulsating iris is used to force a periodic vortical excitation of the flow around an air jet issuing from a nozzle, as the first step of a microgravity diffusion flame experiment. Two different iris models were used with the same jet and flow rate, the second iris being larger than the first. The steady and periodic flowfields are visualized using laser Mie scattering and measured using laser Doppler velocimetry to provide a test case for developing flame computations. Steady, periodic, and non-periodic parts of the three components of velocity fluctuation have been measured. Spectra of velocity components have been acquired, the bulk of the measurements being on the large iris. This report describes experimental configurations, verification procedures, measurement grids, file formats and sample data. Due to the bulk of the data, and the fact that the data on the first iris were sent to SAIC earlier, the data are transmitted and stored electronically.

Introduction

This report describes the acquisition of velocity measurements in a coled air jet flow modulated by a pulsating iris. These measurements serve to define the nonreacting flow. These are a prelude to Drop Tower tests of a burner to study combustion in large-scale vortical structures under microgravity conditions. A camera iris is used as a simple means of generating precisely repeatable periodic oscillations. In the Drop Tower tests, this will be used to create large vortical structures to study a laminar diffusion flame. The cold flow configuration consists of a central jet surrounded by the iris aperture which contracts and dilates, as shown in Fig. 1. The purpose of the iris cold-flow characterization experiment is to validate the iris concept as a means of generating the desired flowfield, and then to define the flow sufficiently to enable development and validation of computational models being developed for the combustion experiment.

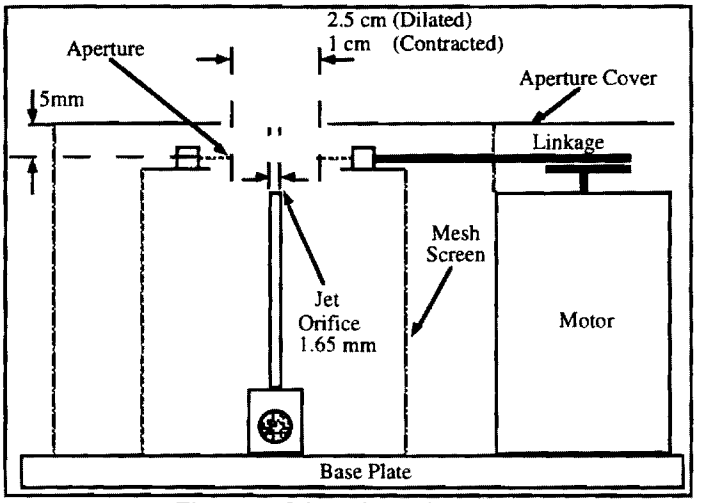

Figure 1: Iris and nozzle set up.

The data consist of phase-resolved velocity measurements taken in the vicinity of the aperture, and supplemented by velocity spectra at selected locations. In addition, laser sheet flow visualization was used to capture the features of the flow both qualitatively and quantitatively.

Experimental Method

Iris Control/ Data Collection

Figure 2 shows the iris control and data collection system.

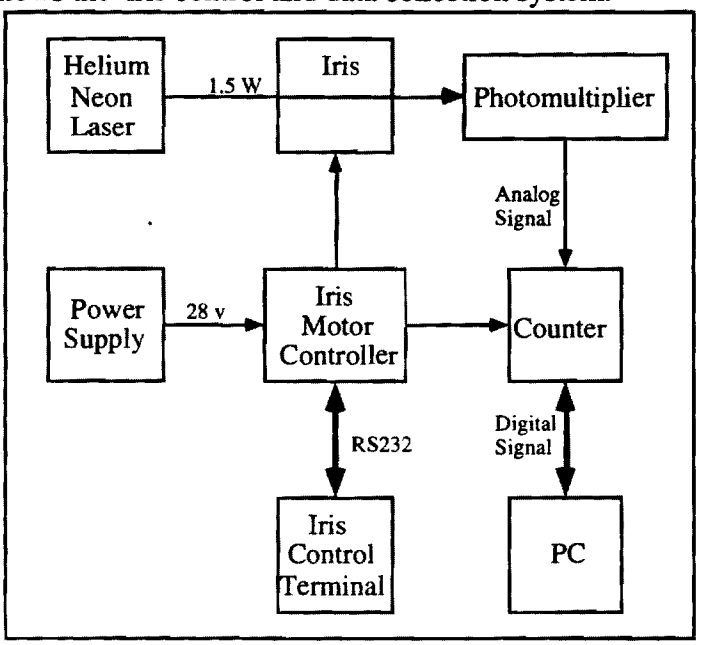

LDV System

The data collection system was centered around a TSI laser Doppler velocimeter (LDV) system and a Spectra Physics 35mw Helium Neon Laser. The light was split into shifted and unshifted beams, steered to intersect in the measuring volume. Scattered light from seed particles traversing the measuring volume is collected into a photomultiplier whose output is directed into a frequency downmixer and thence to the counter processor. The counter takes the signal from the photomultiplier and the trigger pulse signal from the iris and converts the information into a digital form which is then processed and stored by a 33MHz i486 type PC. Note that the trigger from the iris itself was not satisfactory for input into the counter. Thus, the trigger signal from the iris was used to trigger a pulse generator which, in turn, generated a sharp-edged pulse that was used as the input signal for the counter. Also, the trigger occurs at the iris maximum open position, thus zero degrees azimuth corresponds to the fully dilated iris position. The iris power supply was a standard variable voltage unit rated at one Ampere maximum current output. The iris control terminal was a i286 type machine which sent ASCII characters to the iris motor controller via an RS232 serial port. The frequency shift frequency for all data collected during this project was 100 KHz. This frequency was chosen because it is high enough to measure the velocities encountered in the jet, yet low enough that not a great deal of high frequency noise is present in the signal. Other pertinent counter parameters used during data collection are listed below.

Low Filter Limit	30 kHz
High Filter Limit	300kHz
Counter Gain	2
Cycles/Burst	2^3
Comparison Timer	1%
$\Delta\tau$/ Interval	2^6 μs/ step

Table 1: Counter Settings

Data Collection Programs

Three programs were used to collect data. Program "LDVFA" was used to collect freestream (0 Hz) velocity statistics, "LDVIRIS" was used to collect pulsating-flow data, phase-syncrhonized with the iris, and "SPECTRA5" was used to collect velocity spectra using Fast Fourier Transforms (FFTs). All are programs developed in-house, and have seen extensive use in other research projects.

LDVFA

This program collects data from the TSI 1990B LDV counter via a TSI 6260 data interface card, in 5 blocks of 10,000 validated velocity measurements at each location, computes the arithmetic mean and RMS velocities, and computes a velocity histogram. Each data value from the counter consists of the time taken for N cycles of the Doppler shift signal, where N is a preset number, usually 8 or 16 depending on the data arrival rate. The program includes automated movement of the measuring location to each point in a pre-specified grid.

LDVIRIS

This program uses a trigger pulse from the iris mechanism, directed to the interface of the LDV counter processor. Each data word from the counter is accompanied by a word giving the Time Between Data Points, which is the interval since the arrival of the previous value. The first data point to arrive after a trigger pulse is flagged, and carries the time since the trigger pulse. This enables computation of the phase of the iris motion corresponding to the time of arrival of each velocity value. Data are sorted according to the arrival phase into bins with 1-degree phase resolution. At the end of data acquisition, when the specified total number of points has been acquired for that measuring location, the average and the root-mean-square of the values in each bin are computed. For flows such as those in the present experiment, the distribution of data points among bins should be fairly uniform, except that more points are likely to be measured in bins where the velocity is high. The first few points that arrive before the first trigger pulse in each 10000-point block must be discarded because there is no way to know the iris phase at their arrival. Thus each of the 360 bins should have roughly 130 points. The average over the bin is thus the periodic component of the velocity, and the root-mean-square includes any non-periodic variations plus the effect of the velocity gradient across the bin and the random measurement noise. The gradient of the periodic velocity across each bin is expected to be very small, so there is no velocity bias error in performing an arithmetic average of the points in each bin. The mean velocity at the measurement location is the arithmetic average of the bin averages. Thus all effects of velocity bias are avoided. This program also has an automated data acquisition-traversing subroutine.

SPECTRA5

This computes velocity spectra using samples equi-spaced in time, and a standard fast FFT algorithm. To perform equi-spaced sampling, the randomly-arriving data are converted to an analog voltage proportional to the Doppler frequency. The exponent of the data values is fixed to generate consistent voltage variations. The voltage is high-pass filtered with a setting of 0.1 Hz, amplified using a selected gain and low-pass filtered at 20 Hz setting of 20Hz before being taken into a sample-and-hold analog-digital converter. The sampling parameters are chosen to ensure 0.1Hz frequency resolution and a Nyquist frequency above 25Hz. The program compensates for the gain before computing spectra.

Spectra System

The analog signal from the LDV counter is filtered and amplified before sending it to the sample-and-hold interface which is connected to a PC equipped with an analog-digital converter. The "SPECTRA5" program collected 20 blocks with 512 data samples in each and performed an FFT-based spectrum computation. This gives the auto-spectral density of the input signal.

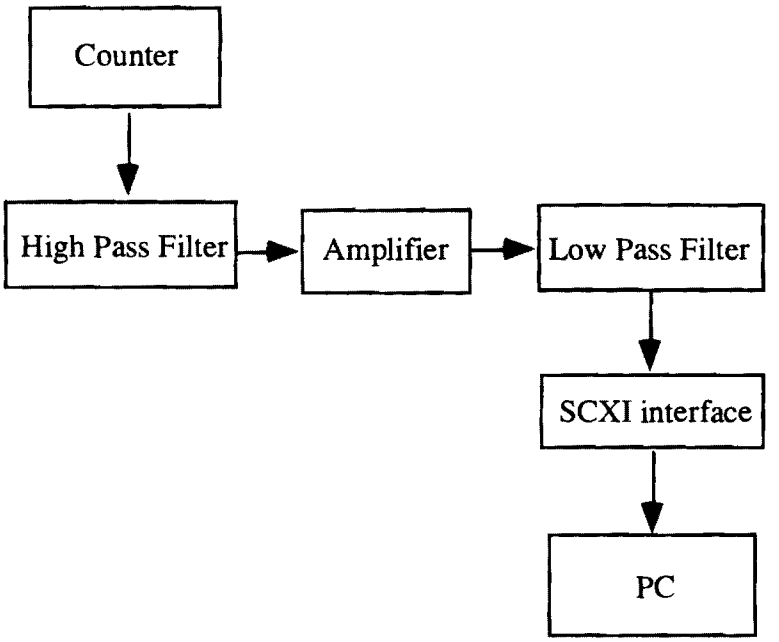

The settings for the filters and amplifier are listed below :

High Pass Filter Setting	0.1 Hertz
Low Pass Filter Setting	20 Hertz
Amplifier Gain	100

Table 2: Spectra Settings

The frequency range set is not only sufficient to capture phenomena occuring at iris pulsing frequencies (2.5,5.0 & 7.5 Hz) but also those substantially above and below the iris frequency. A few tests were also performed with a much higher Nyquist frequency and a low-pass filter set at 500Hz to ensure that no high-frequency phenomena were present.

Environmental Isolation

The measurements on the smaller iris model, reported previously, were performed inside a 1.05m x 1.05m x 2m enclosure built in the test section of the 42" x 42" low speed wind tunnel. For measurements on the larger iris, we constructed a styrofoam enclosure 1m x 0.75m x 0.75m, with plastic sheets sealing off the aperture needed for the LDV system to move during measurements. This was located in the undergraduate fluid dynamics laboratory in Rm 405 of the Aerospace Engineering building. Since no measurements were made during operation of any of the noisier equipment in the lab, background acoustic levels were below 70dB for all of the data acquisition, with no spectral peaks of any significance.

Iris Motor Isolation

There has been some concern that waste heat from the iris drive motor could have a significant effect on the velocity measurements due to convective currents. The motor is located within 8 cm of the iris. To asses the effects of the motor waste heat on the flow field, the mean axial velocity was measured at 17 stations at equal intervals along a diameter from x = -1.5 to 1.5 cm, at z = 1.5 cm above the iris plane (see Fig 3).

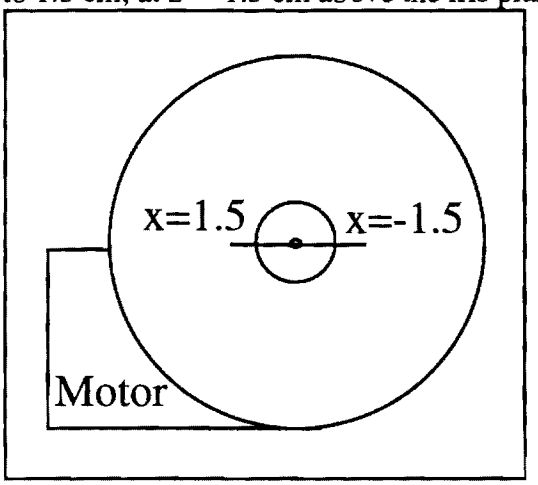

Figure 3: Motor Orientation with Respect to Test Points.

Next, the iris motor coils were energized and allowed to warm up (i.e.- the motor controller was turned on, but no commands were issued to it), and the survey was repeated. The alignment of the measuring volume for these tests is only accurate to +/- 1.5 mm for the data files associated with this test.

Temperature-sensitive liquid crystal sheet was laid over the top of the set-up with a cutout for the iris apearture, and images of color (temperature) distributions were captured using an Apple Quicktake digital camera. The sheet used in these tests was sensitive over a range from 25-30° Celsius.

Results

The velocity measurements are shown in Fig 4, for different warm-up times of the motor. Note the asymmetry in the velocity profile. The iris motor is located to the right of

the rightmost point of the graph suggesting that motor convective currents are the cause of the asymmetry..

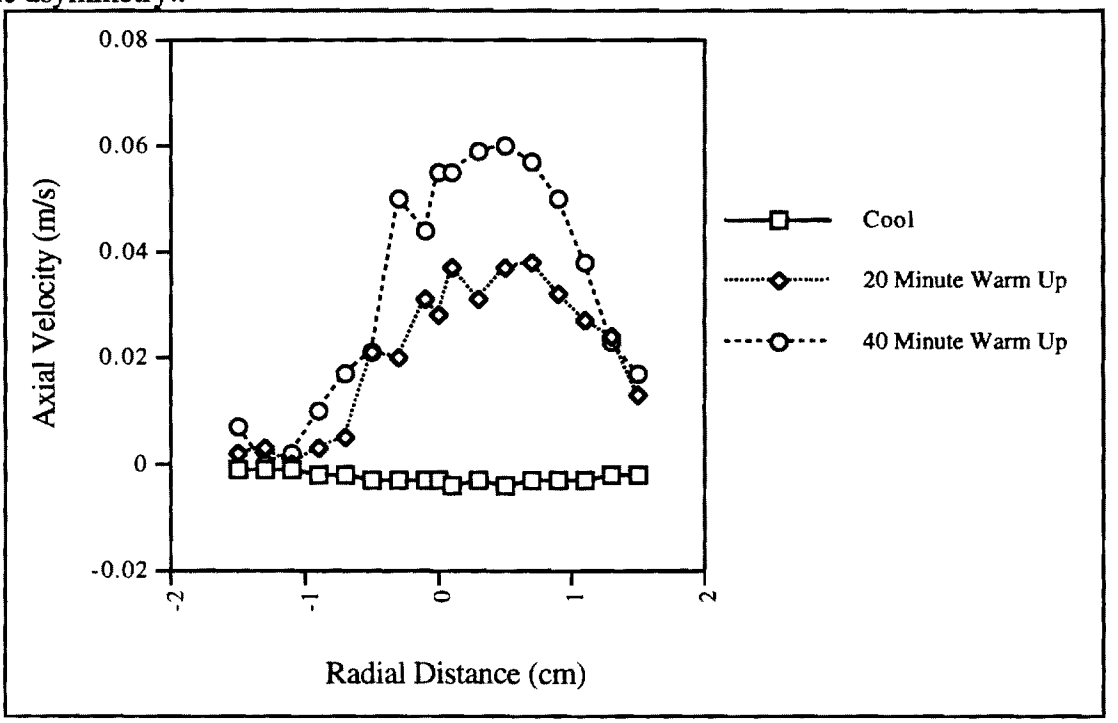

Figure 4: Axial Velocities as Traversed Across the Iris Cover.
Note that the Rightmost Points are Closest to the Motor.

Using liquid crystal visualization, we found that the base plate, iris ring and support are all heated by several degrees Celsius above ambient temperature due to conduction from the drive motor. These thermal gradients near the jet are likely to cause significant convective currents in the measuring grid. In effect, the motor heats the entire unit several degrees above ambient temperature, making thermal isolation difficult because the entire unit must be shielded from the grid.

Corrective Measures

Two approaches were followed: first to increase conduction of the heat away from the jet, and second to insulate the upper surface of the setup from air. We attached a 5 x 8 x 0.3 cm copper plate to the bottom of the stepper motor to carry waste heat away from the iris and measuring grid. This was effective in disposing of part of the waste heat. Typically, this plate was approximately 30° C when the motor was in operation (24° C = ambient temp.). In order to isolate the base plate, we put a thin styrofoam plate (23 x 30 x 1.5 cm) on top of the base plate (see below figure). This isolated the region of the plate outside the inner screen. Small foam chips inside the screen around the base of the jet served to isolate the portion of the base plate directly under the iris. Together, these two measures isolated the base plate from the measuring grid. The motor was insulated from

the iris region using a housing made of high-density foam core cardboard (see Fig. 5).

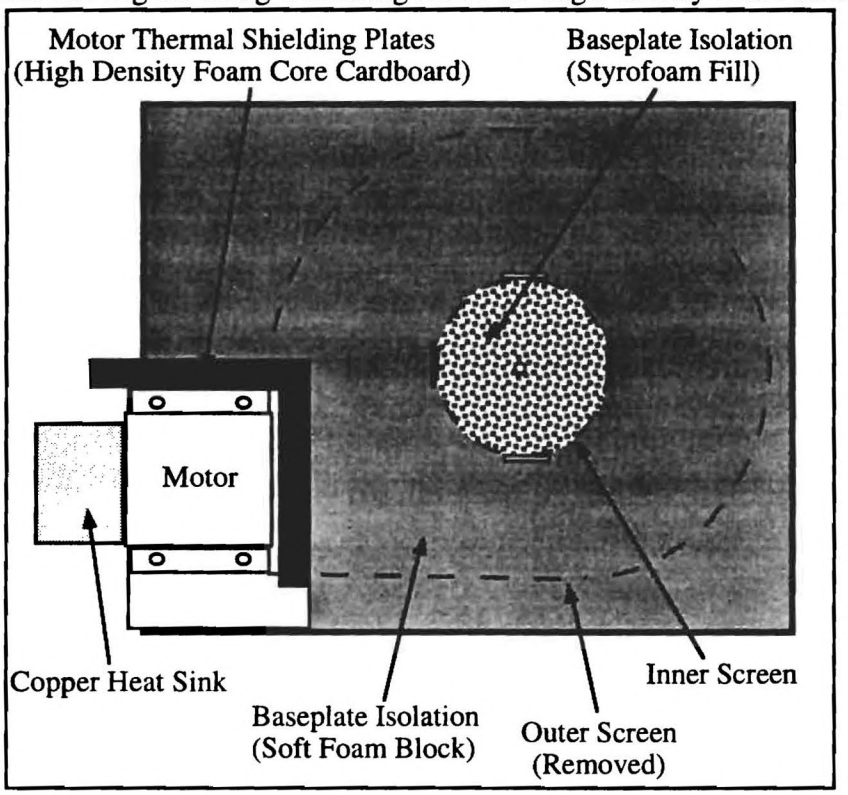

Figure 5: Thermal Insulation Measures.

This left the iris retaining ring and supporting assembly. These are difficult to insulate without modifying the geometry of the configuration. One solution would have been to insert an insulating gasket between the iris support assembly and the base plate in an attempt to prevent heat conduction between the parts. However, this would have required disassembling the iris. We decided against this. The effectiveness of our insulation measures is seen in Fig. 6.

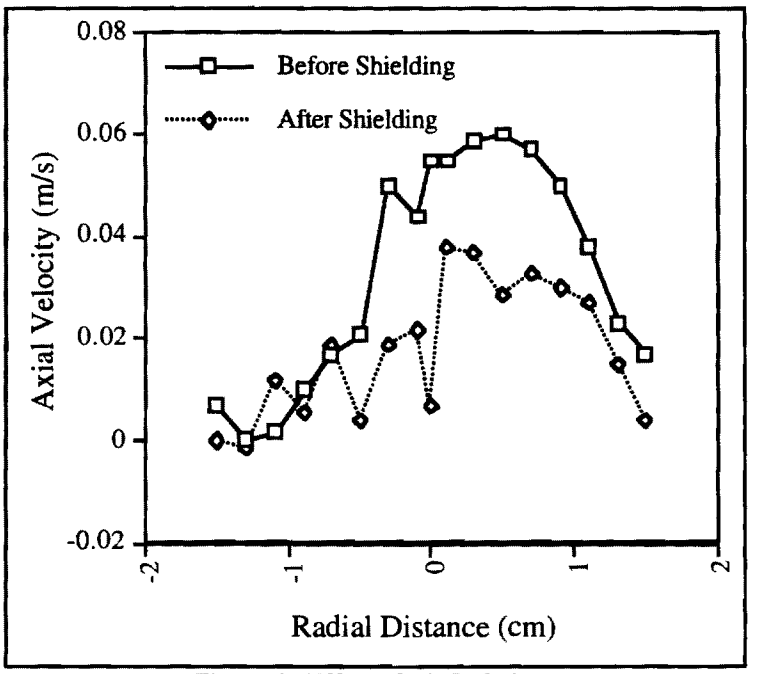

Figure 6: Effect of Iris Isolation.

Finally, we took "before" and "after" pictures of the temperature distribution on top of the iris by using the liquid crystal sheets. These pictures showed that the thermal insulation measures drastically reduced motor waste heat near the grid, and made the temperature distribution much more uniform around the iris.

Conclusions

It is clear that the convective currents from the iris cause at least some asymmetry in the flow. The axial velocities induced by convective currents are on the order of 60 mm/sec maximum before insulation and about 20mm/sec. after. The peak velocity in the core of the jet is of the order of 400 m/s, and the average velocity outside of the jet is on the order of 100 mm/sec. Thus, the thermal currents reach 20% of the velocities achieved from jet interaction. The thermal insulation measures employed have reduced the convective velocities by a factor of 3. This is an improvement over the unshielded setup, and substantially less than that with the previous set-up with the iris cover (used in measurements on the smaller iris) in place. The proximity of the motor to the iris made the task of thermal isolation quite difficult: any active cooling would be impractical, considering that the geometry must not be modified. Hanging the apparatus upside down was considered. In the confined environment of the measurement chamber, this would induce convection currents at the measurement location, which are not expected to be much less than those measured here.

Iris Tilting

The experiment specifications required that the lowest axial coordinate of the measuring grid be .5 cm above the iris plane. However, the iris retaining ring obstructs the laser beam when trying to take axial velocity data at this height, making it impossible to collect data. In order to solve this problem, it was necessary to tilt the iris relative to the LDV by several degrees (see Fig 7). The tilt angle was less than four degrees. The component of axial velocity in the LDV (untilted) reference frame is more than 99% of the absolute magnitude of velocity, thus tilting was considered to have a negligible effect on the magnitude of the velocity measured. Note that iris tilting was necessary only for axial velocity at z = .5 cm stations.

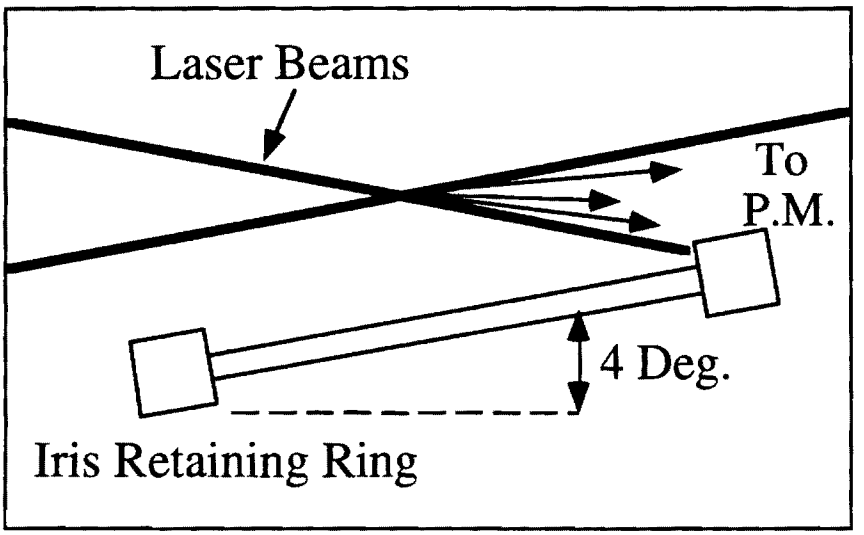

Figure 7: Iris Tilting Setup

Measuring Volume Alignment Using Velocity Profile Data

Measuring volume alignment is critical to measure the of jet core velocity profile. To achieve very fine alignment of the measuring volume with respect to the iris frame, we constructed an "alignment tool" consisting of a pinhole aperture fixed to a rod (see Fig 8). This rod was inserted into the jet pipe and was used to hold the aperture in place. The laser beams were steered such that both beams passed through the aperture simultaneously. This allowed precise location of the measuring volume with respect to the iris mechanism itself.

During the course of data collection, it was necessary to move the iris to a different orientation many times. After each movement, the measuring volume had to be realigned with respect to the iris. By using this simple tool, we could be sure that the measuring volume location was within a fraction of a millimeter of where it was previously.

After the location of the measuring volume with respect to the iris mechanism was known, we took a series of axial velocity data points across the jet. We then used this data to find the centroid of the jet using a code created by U. Reddy. Knowing this offset, we could then find the location of any grid point with respect to the iris or the jet centroid.

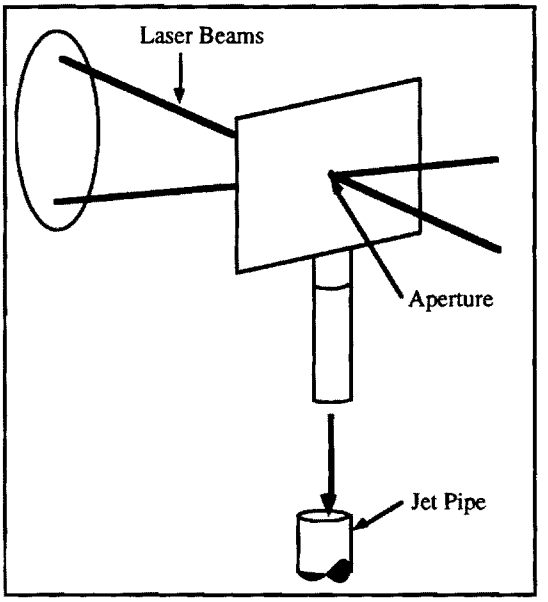

Figure 8: Alignment Tool

Alignment Accuracy and Precision

The diameter of the aperture is approximately .4 mm, while the laser beam diameter was approximately .2 mm. This allowed us to have very accurate alignment in the radial and axial directions, certainly within .3 mm of the desired location. The beam alignment in the tangential direction was less certain using this method, and is approximately $\pm$.4 mm of the desired location.

Traverse Validation

The traverse used to position the measuring volume had stepper motor control in two directions and manual movement in the third. The spatial resolution of the traverse in the directions under computer control are on the order of .01 mm, however, for practical purposes, one should consider the traverse to be accurate to within .1 mm.

The base and the laser platform were leveled. The motorized positioning was verified as follows: Two plumb bobs were suspended from the ceiling of the isolation chamber. The measuring volume was then moved until it was located inside of one of the plumb lines. The traverse was next moved up, causing the measuring volume to rise inside the plumb line. If the measuring volume drifted outside of the plumb line, the traverse was adjusted until this no longer occurred. From the top of the first plumb line, the measuring volume was moved into the top of the second plumb line, downwards along the plumb line, and finally, back to the initial starting place inside the first plumb line. This way, we could be sure that the traverse was moving in a vertical plane. The traverse was moved in this square race track fashion approximately eight times to ensure repeatability of traverse positioning, and to ensure that there is not any significant drift in the traverse positioning after movement.

Fringe Spacing Measurement

Fringe spacing determines the conversion from velocity to the frequency which is measured using the counter. The fringe spacing was found using the equation:

$$d = \frac{\lambda}{\sin(2\theta)}$$

where: d = Fringe Spacing

λ = Wavelength of Laser Light

θ = Beam Half-Angle

The beam half angle was found by measuring the beam separation at the focusing lens and the distance from the lens to the beam crossing (see Figure 9). The laser wavelength is 632.2 nm (Helium-Neon). The fringe spacing was found to be 3.31 micrometers.

Measurements in stagnant air showed that the error in frequency shift and other parameters was less than 0.0008m/s.

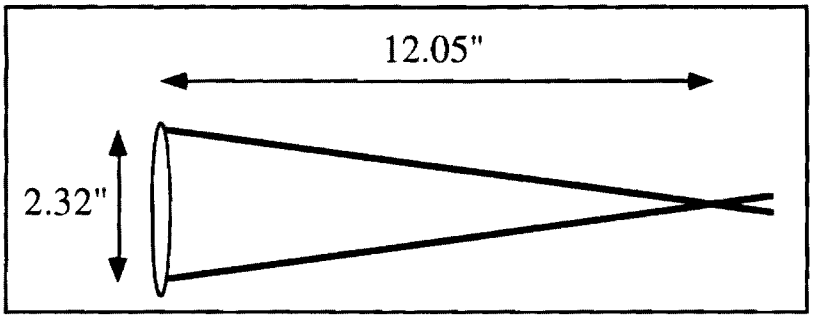

Figure 9: Dimensions Used in Calculation of Fringe Spacing.

Seeding

The air flow is seeded using atomized mineral oil with a nominal droplet diameter of 4 microns. These droplets have a settling velocity which is negligible. After the jet has been operated for a few minutes, the entire isolation chamber is filled with seeded air. There is no danger of pressure increasing in the isolation chamber, because the edges of its walls are not sealed airtight: this is proven by observing the seeded air drifting slowly out. The seeding has to be introduced before the flow goes through the rotameter, which led to some concern about the flowmeter performance as discussed below.

Jet Volume Flow Rate

A primary concern from the start of this project has been the measurement and seeding of the central jet. The primary questions to be answered were:

- Would the seeding drastically effect the flowmeter readings by changing the effective flowtube area when seed particles adhere to the walls?
- Is the flowmeter capable of yielding readings accurate to within several tenths of a milliliter per second?

To address these questions, a simple experiment was conducted. This experiment consisted of two parts: the first addresses the question of seeding in a flowmeter, while the second is concerned with the second question.

The experimental setup is shown in Fig 10. A measuring container was filled with water and placed upside-down in a bucket of water. The flowmeter was set to the desired setting, and its output tube was directed under the inverted measuring container so that the air flow entered the container. The container was then allowed to fill with air until the 1400 mL mark was reached. The time for the container to fill was recorded, and it was then a simple matter to find the actual volume flow rate.

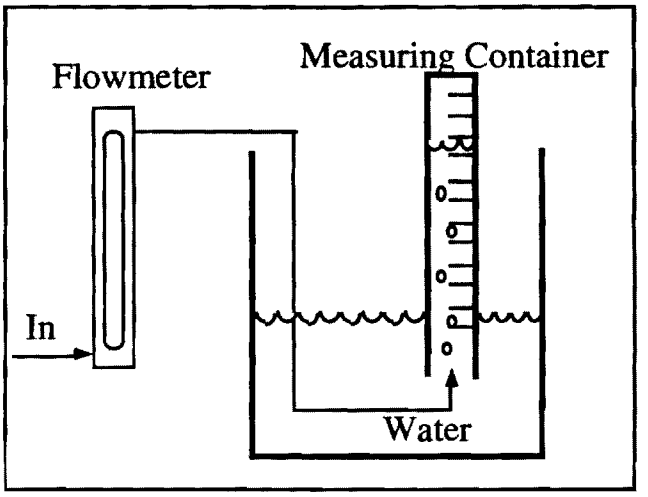

Figure 10: Volume Flow Rate Measurement Apparatus.

Part 1-Particle Interference

The first question addressed is that of seed particle interference. The above experiment was conducted after the flowmeter had undergone several days of heavy use without cleaning. Mineral oil was visible at the bottom of the flow tube, and the float was behaving erratically. The flowmeter was set to give a flow rate of approximately 2.46 mL/sec, and the measuring container was allowed to fill to 1400 mL. The elapsed time to completion was 593 seconds for a volume flow rate of 2.36 mL/sec. Thus the flowmeter reading is verified to stay constant to within 5%, even after extreme exposure to seeding. The flowtube was not allowed to get nearly as "dirty" during data collection as it was allowed to get for this test.

Part 2-Flowmeter Accuracy

In order to test flowmeter accuracy, the flowtube and valve assembly were cleaned using mineral spirits and dried. Next, the same 1400 mL test was conducted with pure air only. The elapsed time for 1400 mL of air to accumulate was 571 seconds to give a volume flow rate of 2.45 mL/sec. Again, these results are very encouraging, with the error being less than 1%.

File Nomenclature

More than 9000 separate data points were collected, each having its own file associated with it. The number of data files in the final data set was reduced to approximately 100 through data postprocessing. In order to ease the task of finding the file associated with a given data point, a simple file naming scheme was adopted. All file names consist of one letter, followed by two numbers, a number/ letter combination, a letter, and a file extension. The Fig 11 shows a typical file name and the meaning of each character in the name.

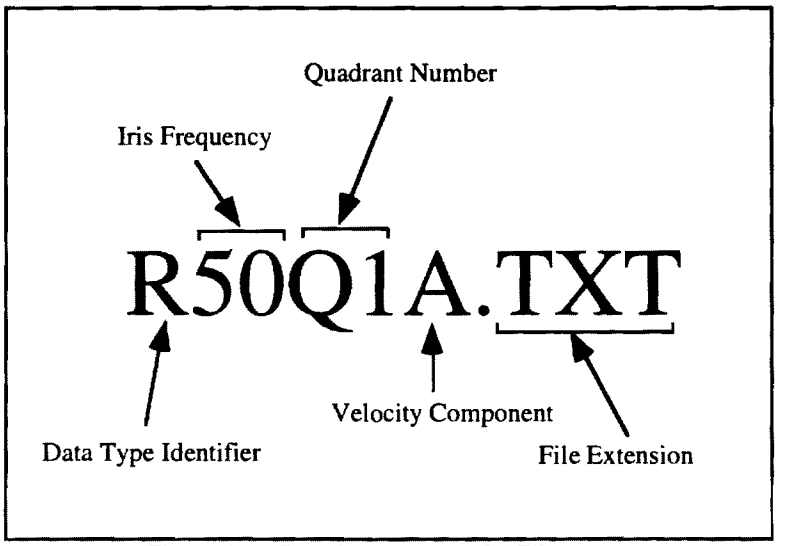

Figure 11: Constituent Parts of a File Name

The first letter in the file name denotes the data type. The letter "R" indicates that the data file was created by the "LDVIRIS" or "LDVFA" data acquisition programs and contains information for a point on the grid in the pulsating mode with the jet turned on. The letter "P" denotes no-jet, pulsating case velocity data, the letter "R" denotes normal motor on, pulsating data, while the letter "N" denotes velocity data taken with the iris motor off. Similarly, for the spectral data, "S" denotes normal "motor on" pulsating spectrum data, the letter "T" indicates no jet spectra, and the letter "U" denotes motor off spectra. This is summarized in Table 2.

Data Type Identifier	Meaning
R	Motor On Velocity Data
N	Motor Cool Velocity Data
P	No-Jet Velocity Data
S	Motor On Spectral Data
T	No-Jet Spectra
U	Motor Cool Spectra

Table 2: Valid Data Type Identifiers

The second and third characters are numbers. They indicate the iris frequency for the data point. This is relatively self-explanatory, with 00 denoting zero hertz, 25 indicating 2.5 hertz, 50, and 75 indicating the higher iris frequencies respectively. The fourth character is "Q" (for quadrant) followed by a number. There are four planes of data at each frequency. Thus, the numbers range from 1-4 designating quadrants 1-4 respectively. See Fig 12 for a diagram of quadrant lines. The sixth digit indicates the velocity component. Again, this is self-explanatory, with the possibilities being **A**xial, **R**adial, and **T**angential.

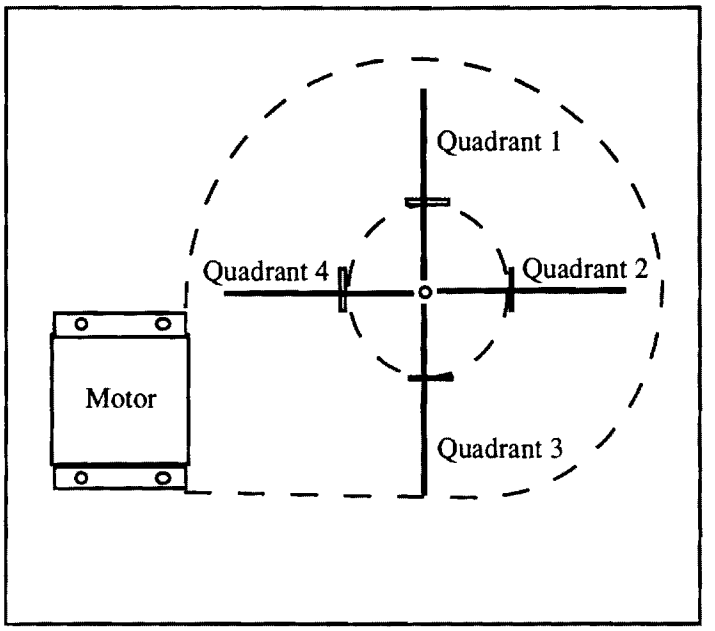

Figure 12: Quadrant Numbering Scheme.

Each of the data files described above contains the data for a block of 91 data points. Depending on the data set accompanying this document, there may be a seventh and eighth digit in the data files (see "Single Point Format" below). These make up the grid point designator. All of the data points measured were located on an irregularly-spaced Cartesian grid. This grid consisted of 91 points ranging from .5 cm up to 4 cm in the axial direction, and from 0 to 2 cm in the radial direction. Each grid point was assigned a grid point designation number, as shown in Fig 13 below. The numbers start at 01 in the core of the jet, move laterally to 2 cm radial distance, and then proceed to the next axial location and move back towards the jet. This pattern is repeated until point number 91 is reached at 4 cm axial distance and 2 cm radial distance (in fact, this is the order in which the data points were collected). These 91 points are the standard set of grid points for which measurements were taken at a variety of frequencies, quadrants, and velocity components.

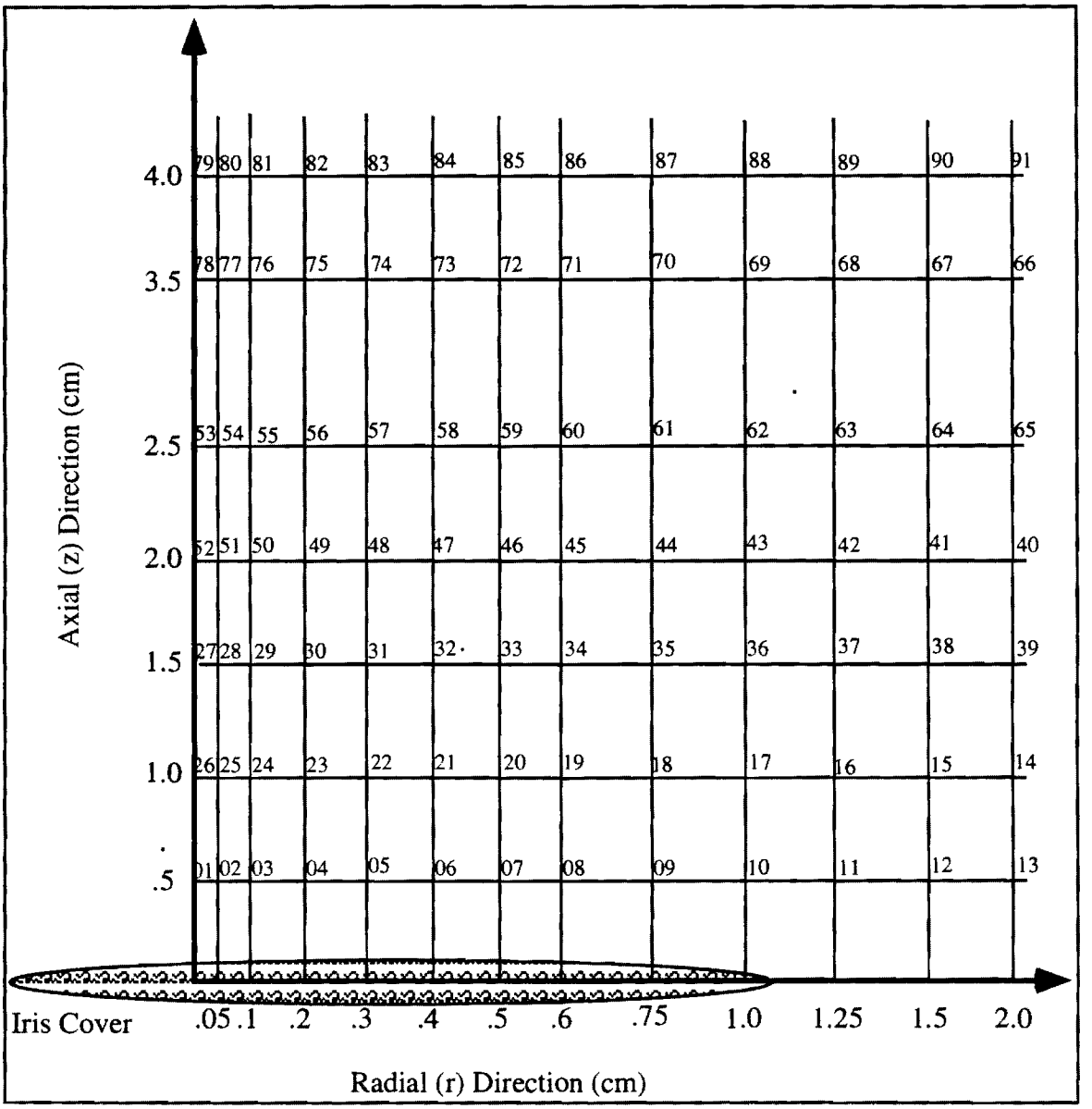

Figure 13: Grid Point Numbering

Data File Structure

As mentioned earlier, the data can be distributed in two forms: the first is data compiled into blocks of 91 data points each, the second consists of one data file for each data point.

Block Format

The 91 data point block format has three file types: that associated with the zero hertz data, that associated with velocity spectrum data, and that associated with the oscillatory data. This was necessary because the oscillating data contains another dimension of data (azimuth) making the data somewhat different from the non-fluctuating data. All files are stored in PC text file format. For examples of data files in the block format, see Appendix A.

The zero hertz data is stored in four columns, with 91 rows (each row containing the information for one data point). The first column contains the radial coordinate, while the second column contains the axial coordinate (see "Iris Orientation and Sign Conventions"). The third column contains the mean velocity, and the fourth column contains the RMS velocity at that point.

The oscillating iris data are stored in six columns, in a similar way to that of the zero Hertz data, except with an extra coordinate. The first column contains the radial location, the second the axial ordinate. The third is iris azimuth, the fourth mean velocity. Finally, the fifth is the RMS velocity, and the sixth is the fluctuating component of velocity. Since the data at each point has been phase averaged with six degree resolution, there are sixty azimuth bins, and thus, it takes sixty rows to contain all of the velocity data for a single point.

The spectrum data is stored in blocks of 39 points (the size of the spectra measuring grid). The data consists of five columns. The first column contains radial locations, while the second contains axial locations. The third contains the frequency, while the fourth contains the signal voltage. Thus, the spectrum information for one point is contained in many rows.

Single Point Format

The files supplied in single point format have three file structures. The first file structure is that created by the "LDVFA" data acquisition program for freestream (0 hertz) measurements. The second file structure consists of post-processed data files created by the "LDVIRIS" data acquisition program and modified in Microsoft Excel. The third is the data file created by the "SPECTRA5" data acquisition program. All data files are stored in PC text file format. Samples of these three data file formats are shown in Appendix A.

The zero hertz data file structure consists of several header lines giving location information, followed by histogram data. The first line of the header gives the gridpoint location of the measuring volume. The second and third lines give the mean and RMS velocities respectively. The histogram data is located below the header and is organized into two columns. The first column contains velocity bins (in m/s), while the second column contains the percentage of measured velocities which fall within the corresponding velocity bin. The files which are of this structure are the zero hertz data files. Thus, any file which has the form "X00QXXXX.TXT" is of this type (see file naming nomenclature).

All files of the second file type are for the pulsating iris case. The file structure consists of a file header followed by azimuth, mean, RMS, and fluctuating velocity information. The first line of the file header contains the location of the measuring volume, enclosed in quotation marks (a characteristic of Microsoft Excel), while the second and third lines contain the mean velocity and RMS velocity over the entire iris cycle. The azimuth, mean, and RMS data is given below the header in three columns. The first column contains azimuth bins in six degree increments. The second column contains the corresponding mean velocity information for that bin, while the third column contains the RMS information for that same bin.

The spectrum data file consists of five columns. The first row is a data header. The second row contains the radial location in the first column, the axial location in the second, frequency in the third, and signal voltage in the fourth. All rows after the first row contain buffering zeros in the second and third columns followed by velocity bin values and spectrum data. Note that the first column of the file contains buffering zeros.

Iris Orientation and Sign Conventions

The coordinate system employed in traversing from grid point to grid point is of the cylindrical type with its origin at the core of the jet and level with the iris aperture plane. The axial (z) direction is positive above the iris plane, and negative below it. The radial direction is positive outward from the axis of the iris, and the tangential direction is positive in the counter clockwise direction as one is looking down on the iris cover. All iris coordinates are given in centimeters and degrees. Fig 14 illustrates the positive sense of the r, θ, and z directions. Note also that zero degrees azimuth corresponds to the maximum iris open position.

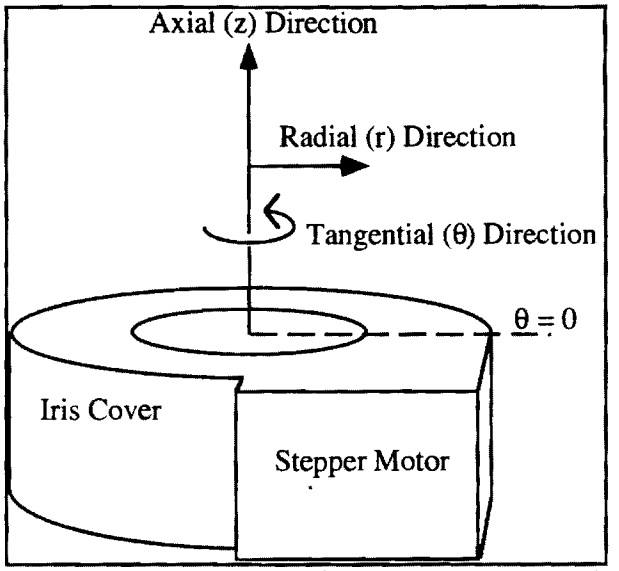

Figure 14: Traverse Coordinate System. All Directions Are Shown in Their Positive Sense.

Test Procedures

As mentioned earlier, the amount of data associated with this project is enormous (relatively speaking), and it was necessary to establish fairly rigid operational procedure in order to ensure data quality and repeatability as well as to eliminate needless errors. An abbreviated version of this is listed in Appendix B.

Initial Setup

The most important aspect of the initial setup was the iris alignment. This is the thing that is most difficult to do consistently. The first step was to put the iris in approximately the right position under the measuring volume, and align the iris in the correct azimuthal (theta) orientation. This was done first because the tolerances for this coordinate were not as stringent as for the radial and axial directions. Next, the iris was moved until the radial and axial directions were very nearly correct, and final alignment was then accomplished using the alignment tool (see "Alignment Method"). This procedure was repeated every time the iris had to be moved to a new theta orientation.

Preparation to Take Block of Data

The first step was to check the iris alignment using the alignment tool. Next, the previous block of data was looked at briefly to confirm that it existed and was reasonable. Next, the input file was prepared for the next run. As mentioned earlier, the data acquisition programs were automated to reduce errors. The program took an input file containing locations and file names and used it to collect data. Next, the isolation chamber was filled with mineral oil seed until the particle density yielded a good data rate. The air in the chamber was then allowed to settle for several seconds before beginning data collection.

Data Postprocessing

Most of the data postprocessing was performed in Microsoft Excel using macros written for this purpose. The data was subsequently imported into Tecplot and plotted. All data postprocessing was performed on a Pentium machine running at 90 MHz. This machine does indicate the so-called "floating-point division error" according to a test program developed by German researchers and obtained from the electronic bulletin boards: we are not aware of any reason for this to affect the results here.

Zero Hertz Data

The only task necessary in postprocessing the zero hertz data was to compile each block of 91 files into a single file which would be easier to use. An Excel Macro was written for this purpose. It simply opened each file, extracted the axial and radial location, the mean velocity, and the RMS velocity and placed them into the appropriate block file.

Oscillating Data

Data postprocessing for the non-zero Hertz data was more complex than for the zero hertz data. First, the data was reduced from one degree azimuth resolution to six degree azimuth resolution using a weighted average function. This weighted average function weighted the bins according to how many data points were in each bin. Expressed mathematically:

$$v' = \frac{\sum v_i n_i}{\sum n_i}$$

where: v' = Averaged Velocity in New Bin

v_i = Velocity in i^{th} bin

n_i = Number of points in i^{th} bin

where, in this case, i would run from one to six. Thus, the postprocessed data has sixty azimuth bins starting at three degrees azimuth with six degree increments. This azimuth-averaged data from each of the 91 files in a grid block was then inserted into a single "block file" and saved in a manner similar to that of the zero hertz data.

Note on Azimuthal Resolution

We have included raw data files with 1-degree bin resolution, purely to avoid irrecoverable loss of information. The user of the data is encouraged to select a resolution appropriate for the physics of the application: this may be as high as 18 degrees or 36 degrees. Such averaging of several bins will probably improve the consistency of the data by reducing the statistical error.

Vector Plots

Once the data had been assembled into large data files, it was then a simple matter to import the data into Tecplot, a data visualization application. Tecplot was then used to make vector plots of the data which are shown in this final report. Tecplot was run on the same Pentium machine which did the data postprocessing.

It was a simple matter to create vector plots for the non-fluctuating data. These are shown in Appendix D. Each plot shows two blocks simultaneously, thus giving a more complete picture of jet behavior than with one block only. Note that these plots do not show tangential velocity.

It was considerably more difficult to find a way to satisfactorily show a vector plot for the fluctuating data. This is because the azimuth ordinate effectively adds another dimension to the plot. However, one method is to show a vector plot similar to that of the zero Hertz plots, except with all azimuth stations shown simultaneously. This gives a clear picture of the general development of the jet, and also shows the amount of fluctuation at a particular point with azimuth (if the velocity fluctuates drastically at a point, it shows as numerous rays pointing in all directions from a point). These vector plots are shown in Appendix E.

Flow Visualization Data

As mentioned earlier, flow visualization data was collected in order to evaluate the general characteristics of the flowfield around the iris.

Setup

The flow visualization setup was relatively simple. Flow visualization experiments were conducted at several different aperture frequencies and jet volume flow rates. In order to see the vortices formed by the aperture, a laser sheet was placed across the centerline of the jet, and a standard consumer grade video camera was used to record all images. The jet mineral oil seeding system described earlier was used to seed the jet, while the area surrounding the jet was visualized using incense sticks. Since the incense sticks produce smoke by burning, all flow visualization data collected using this method is necessarily changed somewhat by the presence of buoyant forces. Thus, the flow visualization data presented in this paper should be viewed primarily as qualitative in nature.

Appendix A: Sample Data

The following is a sample of the output of each of the three data acquisition programs used to collect the data for this project. Note that only the first few lines of each output file are given (for brevity).

Single Point Format

LDVFA

x = 0.400, z = 4.000
Mean Velocity = 0.009427
Velocity = 0.005229

Histogram data	-0.53130	0.00000
	-0.51081	0.00000
	-0.49031	0.00000
	-0.46982	0.00000
	-0.44933	0.00000
	-0.42884	0.00000
	-0.40834	0.00000
	-0.38785	0.00000
	-0.36736	0.00000
	-0.34686	0.00000
	-0.32637	0.00000
	-0.30588	0.00000
	-0.28538	0.00000

...and so on. Column one is velocity bin values (m/s); column two is percentage of points within that bin.

LDVIRIS

x=1, z=2

Azimuth	Vel	RMS	Ptsperbin
0	0.25229	0.12267	91
1	0.25691	0.07784	149
2	0.25193	0.06842	164
3	0.24119	0.09054	142
4	0.26067	0.06942	120
5	0.26625	0.06446	120
6	0.24615	0.07831	160
7	0.26410	0.08828	156
8	0.26511	0.07843	150
9	0.26880	0.07331	137
10	0.24095	0.07294	73
11	0.24587	0.08036	151
12	0.25616	0.08039	166
13	0.25865	0.07828	133
14	0.24714	0.08048	135
15	0.26131	0.07740	126
16	0.26517	0.06500	106
17	0.25346	0.06388	118
18	0.24255	0.08719	144

...and so on.

SPECTRA5

*

Chan	Mean	Freq	AS-Chan 0	
1	0			
0	-0.006529	0.1083	0.00	0.00184

0	0	0	1.00	0.0001226
0	0	0	2.00	6.196e-05
0	0	0	3.00	5.902e-05
0	0	0	4.00	5.972e-05
0	0	0	5.00	9.717e-05
0	0	0	6.00	9.762e-05
0	0	0	7.00	0.0001557
0	0	0	8.00	0.0001633
0	0	0	9.00	7.666e-05
0	0	0	10.00	5.535e-05
0	0	0	11.00	4.344e-05

...and so on. Note that the zeros in the first three columns are buffering zeros. Column five is the autospectra of the signal (channel 0 in this case).

Block Format

The following is a sample of data in the block format.

LDVIRIS

0	0.5	3	-0.00724	0.005468	-0.00145
0	0.5	9	-0.00671	0.005953	-0.00092
0	0.5	15	-0.00587	0.005181	-8.8E-05
0	0.5	21	-0.00478	0.005473	0.001004
0	0.5	27	-0.00582	0.005046	-3.6E-05
0	0.5	33	-0.00885	0.005623	-0.00307
0	0.5	39	-0.00582	0.006462	-3.9E-05
0	0.5	45	-0.00551	0.006676	0.000275
0	0.5	51	-0.00579	0.006491	-6.9E-06

...and so on. The order is: Radial location (cm), axial location (cm), azimuth (degrees), mean velocity (m/s), velocity (m/s), and fluctuating component of velocity (m/s).

LDVFA

0	0.5	-.092	0.002662
0.05	0.	-0.049	0.002631
0.1	0.5	-0.0848	0.002096
0.2	0.5	-0.1194	0.001315
0.3	0.5	-0.1245	0.000809
0.4	0.5	-0.1103	0.00092
0.5	0.5	-0.1046	0.000783

... and so on. The order is: Radial Location (cm), axial location (cm), mean velocity (m/s), velocity (m/s).

SPECTRA5

(Insert data file here.)

Appendix B: Operational Procedure (Abbreviated)

Initial Setup

- Turn equipment on.
- Turn shop air on
- Turn iris on and allow to warm until motor temperature reaches 31° C.
- Adjust flowmeter to desired volume flow rate.
    - Confirm that settling chamber (bucket) is well sealed.
    - Use Control Panel as a course adjustment.
    - Use flowmeter valve as fine adjustment.
    - Confirm that float is at desired position 1 minute after final adjustment.
- Align the measuring volume.
    - Make sure iris is in correct theta orientation (3 degree tolerance).
    - Move traverse and/or iris until measuring volume is approximately in jet core (+-2mm).
    - Fine alignment, put alignment tool into jet and align measuring vol. in x dirn(+-.4mm).
    - For z alignment, center beam in alignment tool aperture (+-.4mm).
    - For y alignment, move traverse in +-y directions until beam strength is maximized.
    - Confirm alignment by visually checking that jet goes through center of measuring vol.
- Re-Check Flowmeter reading.
- Begin preparations to take a block of data.

Preparation to Take a Block of Data

- Check that previous block (if any) is valid.
    - Move measuring vol. to origin and visually check that it is in the jet.
    - Select several data files, confirm they were saved with no 0 pts/bin problems.
- Move traverse back to origin.
- Prepare input file for next run.
- Confirm measuring volume alignment (Optional).
    - Move traverse to origin.
    - Confirm x alignment by inserting alignment tool and aligning measuring volume.
- Confirm that iris mechanism is operating properly (green status light, noise, etc).
- Fill isolation chamber with fog and confirm good data rate.
- Begin data collection.

Shutdown

- Confirm that last block was valid as per instructions above.
- Move traverse back to coordinate origin.
- Shut off all equipment.

Appendix C: Experiment Conditions and Specifications

Parameter	Specified Value
Pressure	Atmospheric
Temperature	298K +-
Jet Flow Rate	2.46 cc/sec
Inner Diameter of Nozzle	1.65 mm
Average Velocity of Air at Nozzle Exit	115 cm/sec
Location of Iris Plane Above Nozzle Tip	5 mm
Frequency of Iris Pulses	0, 2.5, 5, 7.5 Hz

Table 3: Specified Experiment Conditions

Measurements:

- z = .5, 1, 1.5, 2, 2.5, 3.5, 4 cm
- r = 0, .05, .1, .2, .3, .4, .5, .6, .75, 1.0, 1.25, 1.5, 2.0 cm
- $\theta = 0^o, 90^o, 180^o, 270^o$
- All three components of velocity.
- Cool, 0Hz, 2.5Hz, 5Hz, 7.5Hz, 5Hz-nojet
- Spectrum at all locations above at axial locations z = .5, 1, 4 cm

Totaling 9360 data points, equivilant to 120 Mbytes of data before postprocessing.

Appendix D: Vector Plots (Zero Hertz Case)

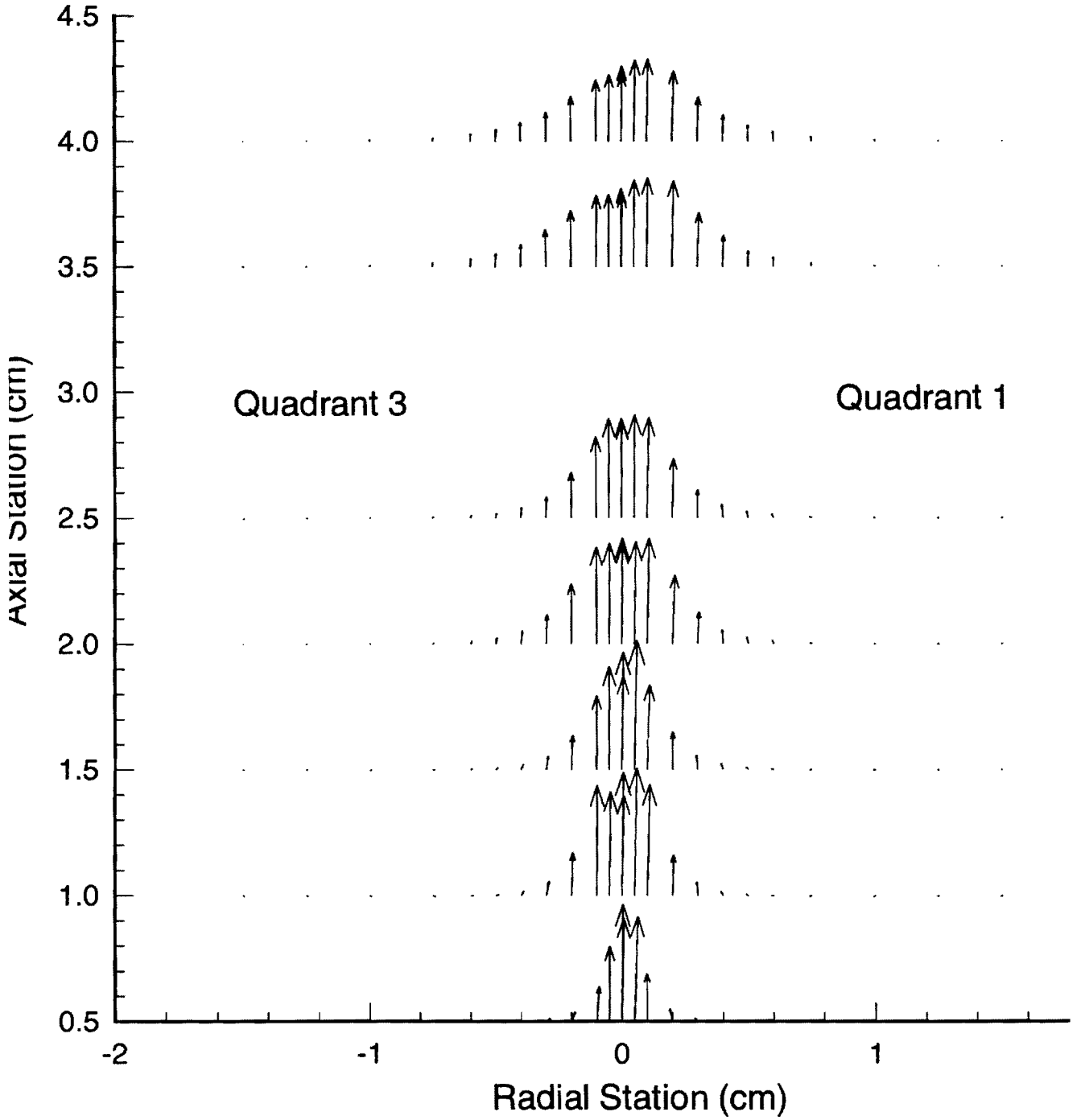

Figure A1: Vector plot for Zero Hertz, Motor Off Case, Quadrants I and III.

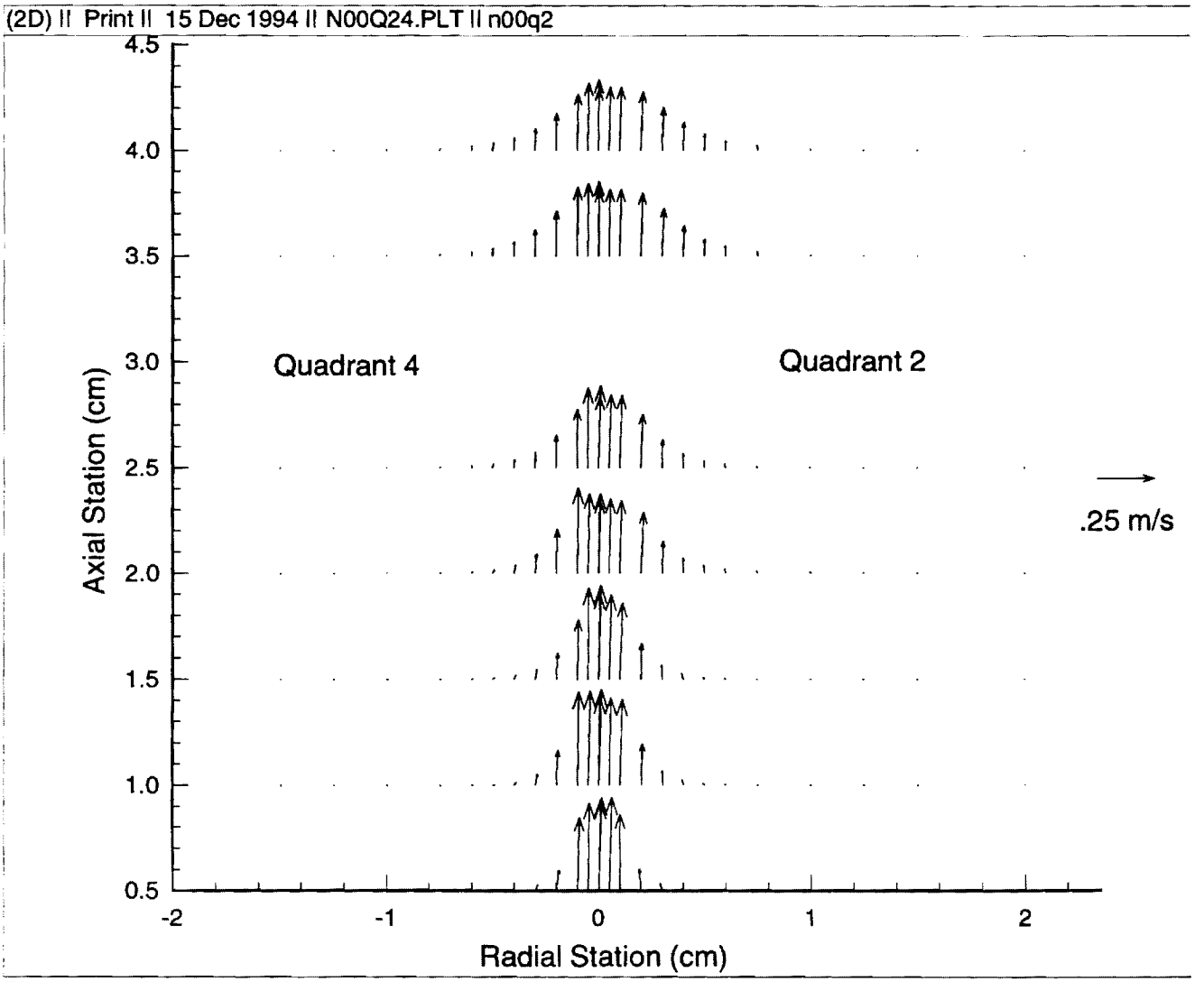

Figure A2: Vector plot for Zero Hertz, Motor Off Case, Quadrants II and IV.

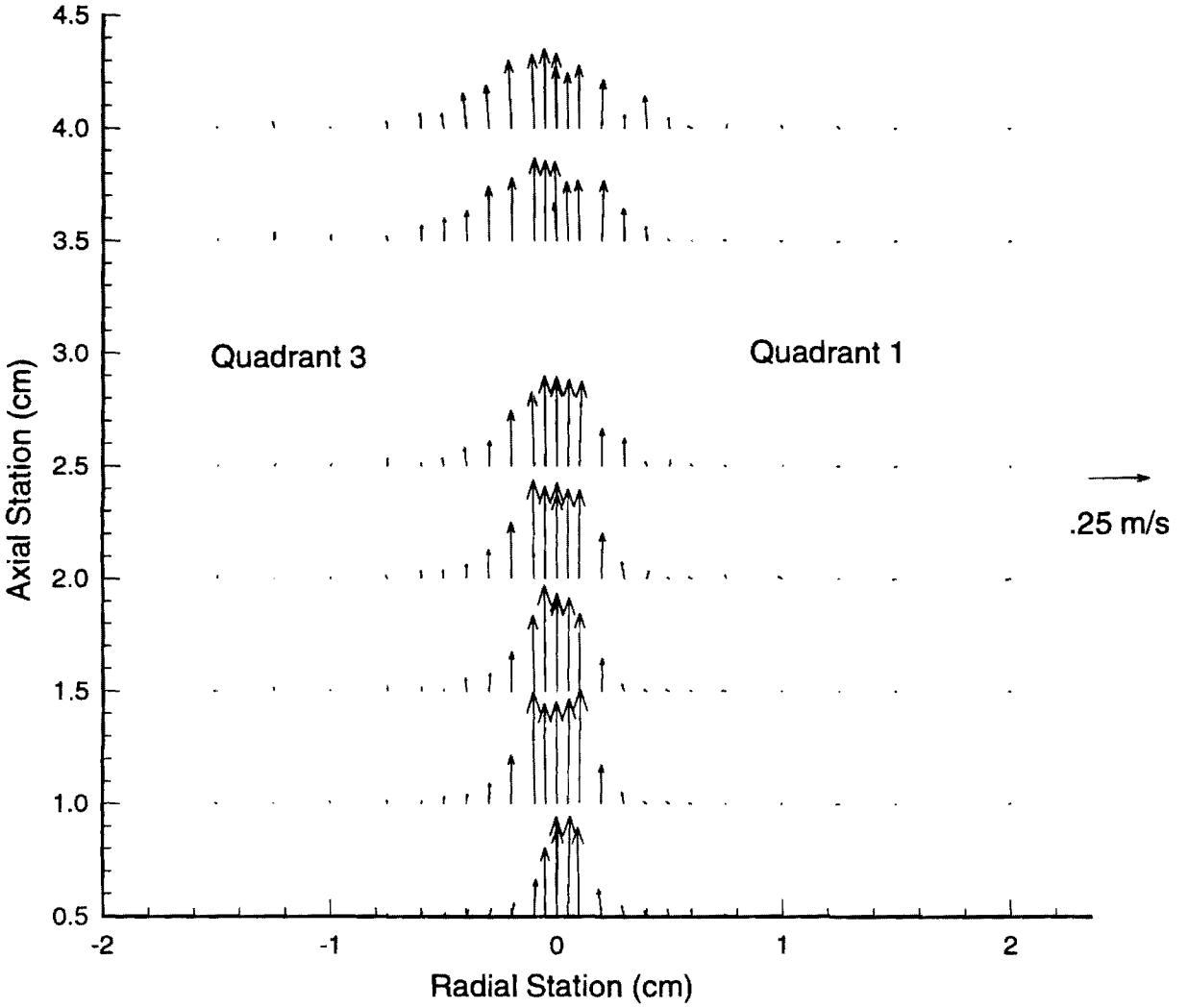

Figure A3: Vector Plot for Zero Hertz, Motor On Case, Quadrants I and III

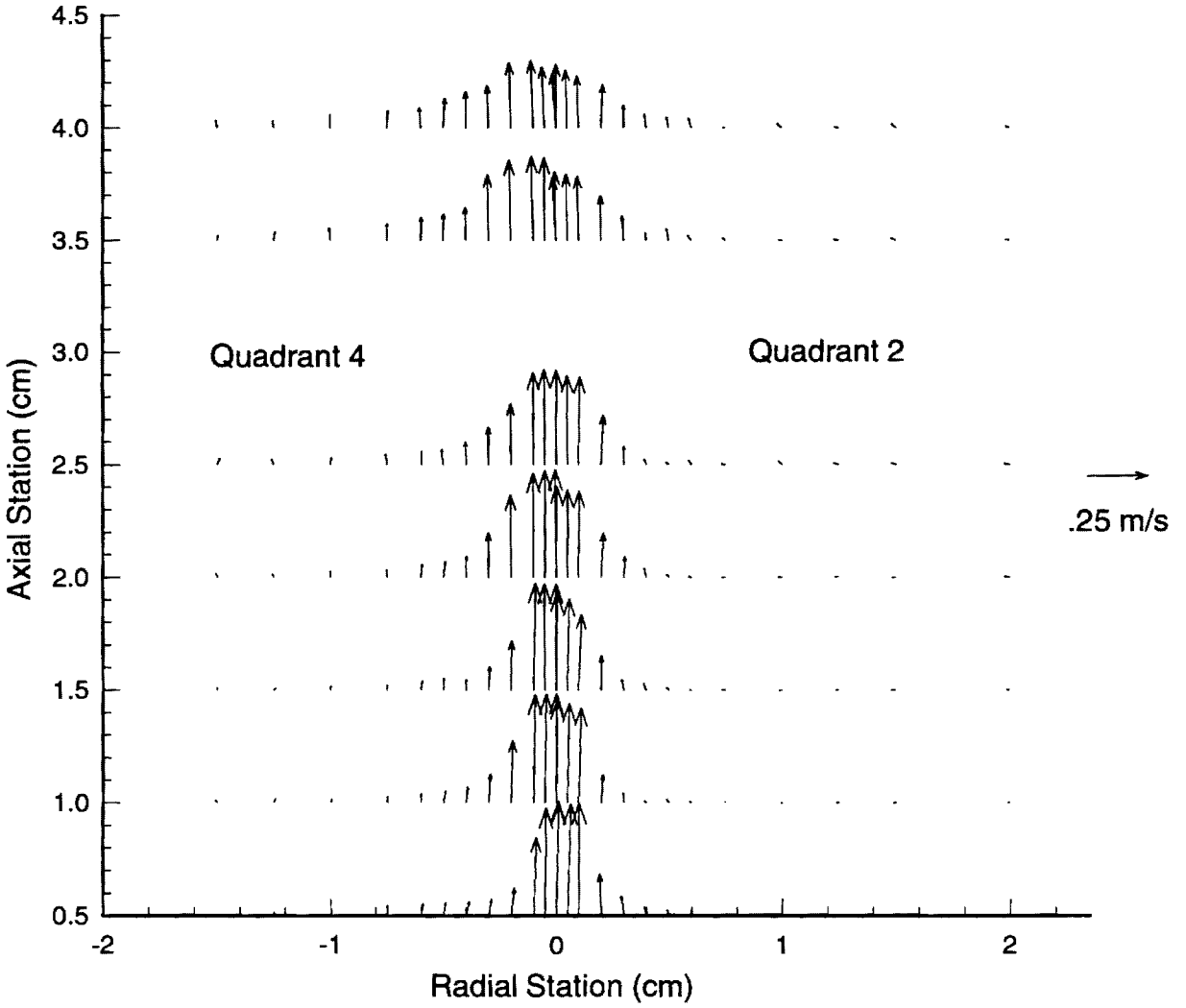

Figure A4: Vector Plots for Zero Hertz, Motor On Case, Quadrants II and IV

Appendix E: Autospectra (Tangential)

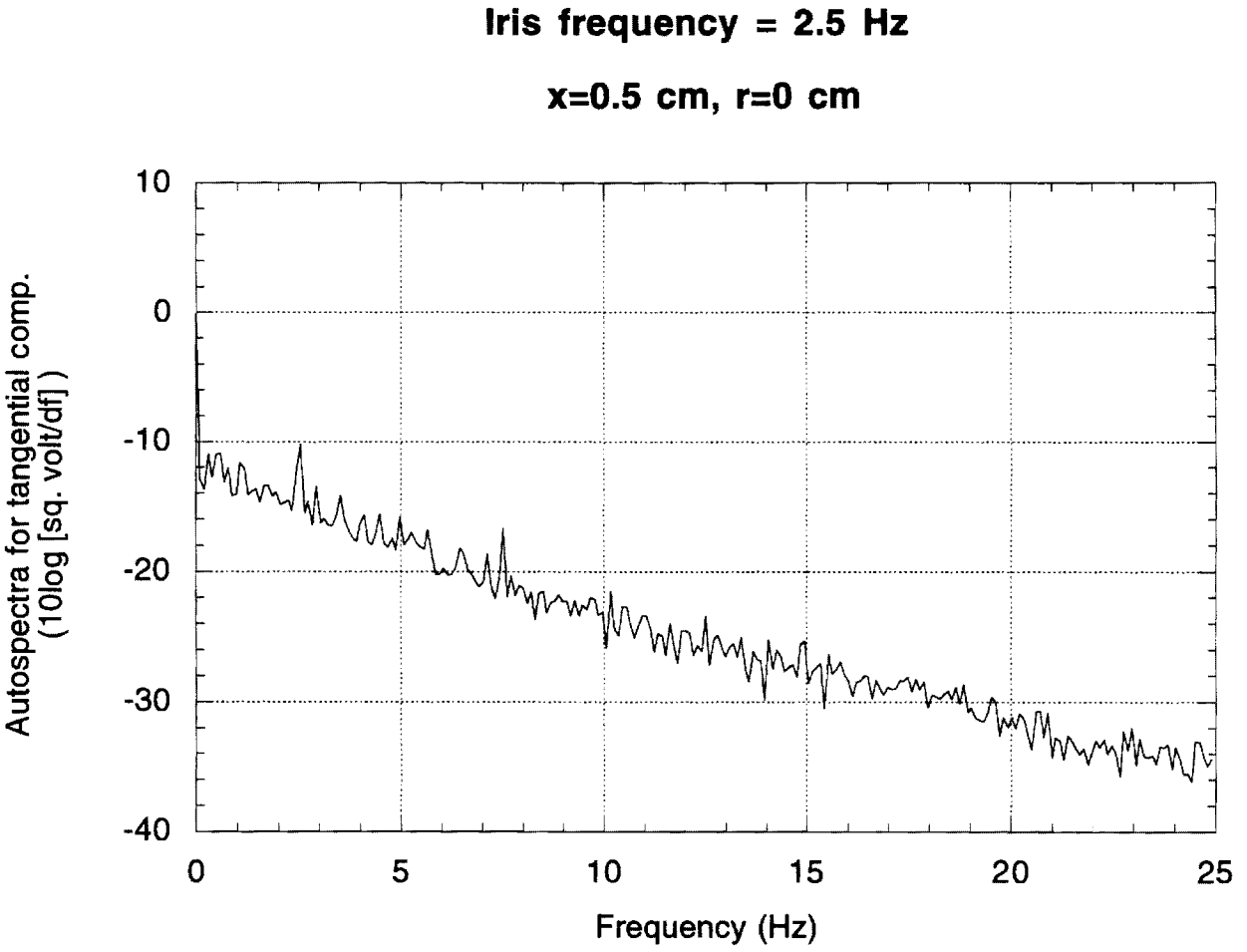

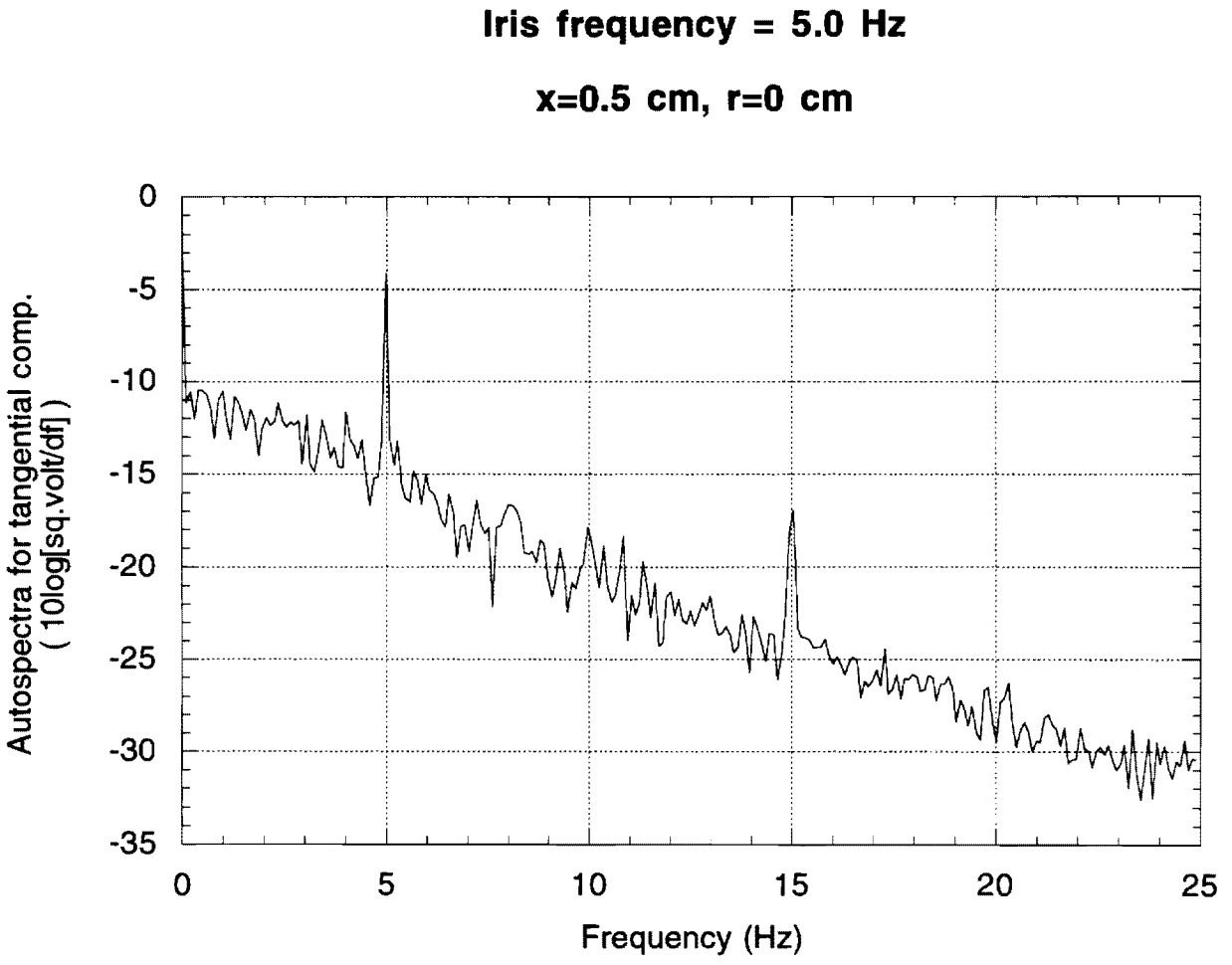
Iris frequency = 5.0 Hz
x=0.5 cm, r=0 cm
Autospectra for tangential comp.
(10log[sq.volt/df])
0
-5
-10
-15
-20
-25
-30
-35
0
5
10
15
20
25
Frequency (Hz)

Appendix F: Flowfield Swirl